

# Infrared photodissociation spectroscopy of $\text{Mg}^+(\text{NH}_3)_n$ ( $n = 3-6$ ). Direct coordination or solvation through hydrogen bonding

Kazuhiko Ohashi<sup>a,\*</sup>, Kazutaka Terabaru<sup>b</sup>, Yoshiya Inokuchi<sup>c,1</sup>,  
Yutaka Mune<sup>b</sup>, Hironobu Machinaga<sup>b</sup>, Nobuyuki Nishi<sup>c</sup>, Hiroshi Sekiya<sup>a</sup>

<sup>a</sup> *Department of Chemistry, Faculty of Sciences, Kyushu University,  
Hakozaki, Fukuoka 812-8581, Japan*

<sup>b</sup> *Department of Molecular Chemistry, Graduate School of Sciences, Kyushu University,  
Hakozaki, Fukuoka 812-8581, Japan*

<sup>c</sup> *Institute for Molecular Science, Myodaiji, Okazaki 444-8585, Japan*

## Abstract

The infrared photodissociation spectra of mass-selected  $\text{Mg}^+(\text{NH}_3)_n$  ( $n = 3-6$ ) are measured and analyzed with the aid of density functional theory calculations. No large frequency reduction is observed for the NH stretches of ammonia, suggesting that either all the ammonia molecules coordinate directly to the  $\text{Mg}^+$  ion or an additional ammonia in the second shell bridges two ammonias in the first shell through hydrogen bonds. Four or possibly five ammonia molecules are allowed to occupy the first shell, in striking contrast to the closure of the first shell in  $\text{Mg}^+(\text{H}_2\text{O})_3$ .

---

\* Corresponding author. Fax: +81-92-642-2607.

*E-mail address:* kazu.scc@mbox.nc.kyushu-u.ac.jp (K. Ohashi).

<sup>1</sup> Present Address: Department of Basic Science, Graduate School of Arts and Sciences, The University of Tokyo, Komaba, Meguro-ku, Tokyo 153-8902, Japan.

## 1. Introduction

Solvation is a phenomenon of fundamental interest in liquid-phase chemistry. The study of clustering processes around an ion in the gas phase enables us to elucidate the ion solvation at molecular level [1]. High-pressure mass spectrometry has been used to obtain the enthalpies and free energies of association as a function of solvent number [2,3], providing insight into the presence of solvent shells. Time-of-flight mass spectrometry [4] and flow-tube studies [3] have also found great utility in identifying solvated ions of unusual stability through the observation of magic numbers. More detailed information on the ion solvation has become available through spectroscopic studies of solvated ions. Vibrational spectroscopy of singly-charged alkali metal ions solvated by H<sub>2</sub>O and CH<sub>3</sub>OH has furnished evidence for the formation of the second solvation shell before the complete filling of the first shell [5]. Solvation structures and dynamics around transition metal ions have also been studied by combination of laser vaporization methods with infrared (IR) photodissociation spectroscopy [6,7]. Electronic spectroscopy has been applied to singly-charged alkaline earth metals solvated by polar molecules, since the electronic transitions of the single valence electron offer a convenient probe of the local solvation environment around the metal ion [8,9].

The Mg<sup>+</sup>(NH<sub>3</sub>)<sub>n</sub> system has received significant experimental and theoretical attention. Bauschlicher and co-workers [10,11] carried out extensive theoretical calculations to predict the geometrical structure, binding energy, and vertical transition energies for  $n = 1$ . Bohme and co-workers [12–14] reported the kinetics of the sequential solvation of Mg<sup>+</sup> with ammonia molecules and the energetics was also followed by density functional theory (DFT) calculations. Stepwise binding energies were determined in collision-induced dissociation (CID) experiments with supporting *ab initio* calculations by Armentrout and co-workers [15]. Soep and co-workers [16] performed DFT calculations of Mg<sup>+</sup>(NH<sub>3</sub>)<sub>n</sub> in analyzing the ionization energy thresholds of the neutral clusters. Electronic photodissociation spectroscopy of Mg<sup>+</sup>(NH<sub>3</sub>)<sub>n</sub> was reported for  $n = 1-4$  by Fuke and co-workers [17,18] and for  $n = 1-7$  by Farrar and co-workers [9]. The spectra exhibit increasing red shifts with cluster

size up to  $n = 4$ , but the additional ammonia molecules provide only slight perturbations on the lowest-energy feature of the  $n = 4$  spectrum. The observation was interpreted in terms of the closure of the first solvent shell with four ammonia molecules.

In this work, we apply the IR photodissociation spectroscopy to  $\text{Mg}^+(\text{NH}_3)_n$ . The method has capability of probing the solvation structures more directly, since the NH stretches of ammonia are sensitive to changes in its bonding environment. Our aim here is to ascertain whether the closure of the first solvent shell is revealed in the IR spectrum. DFT calculations are also performed to predict minimum-energy structures and corresponding IR spectra of  $\text{Mg}^+(\text{NH}_3)_n$ . The comparison of the experimental and theoretical results provides information on the number of molecules in the first solvent shell.

## 2. Experimental and computational

The IR photodissociation spectra of  $\text{Mg}^+(\text{NH}_3)_n$  ( $n = 3-6$ ) are measured by using a triple quadrupole mass spectrometer [19]. The solvated metal ions are produced in a laser vaporization source. The parent ions of interest are isolated by the first quadrupole mass filter. After deflection by an ion bender, the ions are introduced into the second quadrupole ion guide and irradiated by an IR laser (Continuum, Mirage 3000). The vibrational excitation induces fragmentation of the parent ions. After leaving the ion guide, the fragment ions are analyzed by the third quadrupole mass spectrometer. The spectra of  $\text{Mg}^+(\text{NH}_3)_n$  are obtained by recording the yields of the  $\text{Mg}^+(\text{NH}_3)_{n-1}$  fragment ions as a function of wavenumber of the IR laser.

The energy of a photon in the  $3000-3500 \text{ cm}^{-1}$  region (0.37–0.43 eV) is smaller than the  $\text{Mg}^+(\text{NH}_3)_{n-1}-\text{NH}_3$  ( $n = 1-5$ ) bond dissociation energies determined by Armentrout et al. [15]. Nevertheless we believe that one-photon absorption predominantly contributes to the spectra, since the IR laser is not focused in the present experiment. It follows that we preferentially detect a hot subset of the clusters with internal energies sufficient for the one-photon dissociation. As a result, the spectral features of smaller clusters are fairly broad because of overlapping hot bands. Rare-gas tagging technique is often employed in such a

case, which is capable of decreasing bandwidths without introducing significant spectral shifts [20–23]. We therefore measure the spectra of  $\text{Mg}^+(\text{NH}_3)_n\text{-Ar}$ , when necessary, by monitoring the Ar loss channel.

Theoretical calculations are carried out with GAUSSIAN 98 program package [24] using the hybrid DFT method (B3LYP) with 6-31+G\* basis sets. The main purpose is not to locate all the possible isomers at high levels of theory, but to predict the theoretical IR spectra of the clusters. The geometries of  $\text{Mg}^+(\text{NH}_3)_n$  ( $n = 1\text{--}5$ ) are optimized without any symmetry constraints. The harmonic vibrational frequencies and IR absorption intensities are evaluated for a comparison with the observed spectra. The frequencies of all the vibrations of all the species are scaled with a factor of 0.9569, which is chosen to reproduce the NH stretching frequency ( $\nu_3 = 3444 \text{ cm}^{-1}$ ) of the gas-phase ammonia molecule.

### 3. Results and discussion

#### 3.1. Minimum-energy structures

Fig. 1 shows the structures of  $\text{Mg}^+(\text{NH}_3)_n$  ( $n = 3\text{--}5$ ) optimized at the B3LYP/6-31+G\* level. For a given cluster size, several isomeric structures are found with different distributions of the ammonia molecules in the successive solvation shells. The labeling ( $n_1 + n_2 + \dots$ ) is used to classify these structures, where  $n_i$  is the number of ammonia molecules in the  $i$ th solvent shell. Theoretical calculations have already been carried out for  $n = 1\text{--}3$  at the SCF/TZ2P level by Bauschlicher et al. [10,11], for  $n = 1\text{--}5$  at the MP2/6-31G\* level by Armentrout et al. [15], for  $n = 1\text{--}7$  at the B3LYP/6-31G\* level by Elhanine et al. [16], for  $n = 1\text{--}8$  at the B3LYP/6-31+G(d), B3LYP/DZVP, and higher levels by Hopkinson et al. [12–14], and for  $n = 1\text{--}4$  at the MP2/6-31++G(d,p) level by Fuke et al. [18]. The structures obtained from our calculations are consistent with those reported previously, except as noted below. Since the theoretical results have already been discussed in detail [10–16,18], we only briefly describe the qualitative aspects of our results as well as the previous ones.

Fig. 1a exhibits the results of  $\text{Mg}^+(\text{NH}_3)_3$ . All the three ammonia molecules are directly bonded to  $\text{Mg}^+$  in 3I (3+0). In 3II (2+1), on the other hand, only two ammonias are

bonded to  $\text{Mg}^+$  and the third molecule is hydrogen-bonded to the one in the first shell. The 3s valence electron on  $\text{Mg}^+$  is not involved in the  $\text{Mg}^+-\text{NH}_3$  bonds, but polarized away from the ammonia molecules by mixing in some 3p character [11]. Consequently, all the ammonia molecules are located on the same side of  $\text{Mg}^+$ . The B3LYP and MP2 calculations showed that 3I is more stable than 3II [12,13,16,18].

Fig. 1b illustrates four structures of  $\text{Mg}^+(\text{NH}_3)_4$  examined in this work. Both 4I and 4II are classified as 4+0 structures; 4I has tetrahedral ( $T_d$ ) symmetry, whereas 4II is referred to as a ‘distorted square planar’ form with  $C_{2v}$  symmetry [13]. Meanwhile, both 4III and 4IV are grouped into 3+1 structures; the fourth molecule in 4III is hydrogen-bonded to the one in 3I, whereas two ammonias in 3I are bridged by the fourth molecule through hydrogen bonds in 4IV. The energies of these four structures are similar to each other and the relative stability interchanges depending on the levels of theory employed [12,13,15,16,18]. Other isomers such as 2+2, 2+1+1, 1+3, and 1+1+1+1 structures have also been reported [16,18], but these structures are not included here because they are less stable than structures 4I–4IV [18].

Fig. 1c represents four structures investigated for  $\text{Mg}^+(\text{NH}_3)_5$ . All the five ammonia molecules are directly bonded to  $\text{Mg}^+$  in 5I (5+0), which takes a trigonal bipyramidal form. Armentrout et al. [15] reported that another 5+0 structure with a square pyramidal form was located at the global minimum from their MP2 calculations. However, 5I is found to be the only 5+0 structure from our DFT calculations, as already pointed out by Hopkinson et al. [13]. On the other hand, structures 5II–5IV belong to 4+1 structures. In 5II and 5III, the fifth molecule is hydrogen-bonded to the one in 4I and 4II, respectively, whereas two ammonias in 4II are bridged by the fifth molecule through hydrogen bonds in 5IV.

### 3.2. Photodissociation spectra

Fig. 2 displays the IR photodissociation spectra of  $\text{Mg}^+(\text{NH}_3)_n$  ( $n = 3-6$ ) in the 2600–3600  $\text{cm}^{-1}$  region. The  $n = 3$  spectrum shows broad maxima at 3265 and 3355  $\text{cm}^{-1}$ .

In the  $n = 4$  spectrum, a number of bands appear to overlap each other in the 3000–3500  $\text{cm}^{-1}$  region, producing a continuous background. For  $n = 5$  and 6, the intensity of the fragment ions increases substantially compared to  $n \leq 4$ , resulting in good signal-to-noise ratio spectra. In addition, the width of the bands becomes much narrower. In the  $n = 5$  spectrum, two prominent bands are located at 3095 and 3135  $\text{cm}^{-1}$ . The  $n = 6$  spectrum is surprisingly similar to that of  $n = 5$ . In the following sections, each spectrum in Fig. 2 is compared with the theoretical spectra for the structures presented in Fig. 1.

### 3.3. $\text{Mg}^+(\text{NH}_3)_3$

The theoretical spectrum of 3I (Fig. 3b) exhibits the free NH stretches of the ammonia molecules in the first shell at 3257, 3362, and 3369  $\text{cm}^{-1}$ . In the spectrum of 3II (Fig. 3c), on the other hand, a hydrogen-bonded NH stretch is located at 2880  $\text{cm}^{-1}$  in addition to the free NH stretches in the 3260–3410  $\text{cm}^{-1}$  region. The experimental spectrum (Fig. 3a) shows no appreciable absorption in the region of the hydrogen-bonded NH stretch, indicating that 3II is absent under the present experimental conditions. The theoretical spectrum of 3I reasonably reproduces the experimental spectrum, but the observed bands are broad and overlapping each other. We apply the argon tagging technique to obtain more accurate vibrational frequencies. Fig. 3d represents the spectrum of  $\text{Mg}^+(\text{NH}_3)_3\text{-Ar}$ . The broad features seen in Fig. 3a collapse into sharp bands peaked at 3265, 3360, and 3413  $\text{cm}^{-1}$ . The 3360  $\text{cm}^{-1}$  band corresponds to the 3362 and 3369  $\text{cm}^{-1}$  transitions while the 3265  $\text{cm}^{-1}$  band to the 3257  $\text{cm}^{-1}$  transition in the spectrum of 3I. The weak 3413  $\text{cm}^{-1}$  band is tentatively attributed to a combination band involving an intermolecular vibration.

Thus the IR spectroscopy confirms that all the three ammonia molecules are directly bonded to  $\text{Mg}^+$  in  $\text{Mg}^+(\text{NH}_3)_3$ , which is consistent with the most stable structure obtained from the theoretical calculations [12,13,16,18].

### 3.4. $\text{Mg}^+(\text{NH}_3)_4$

The unresolved features preclude the detailed analysis of the experimental spectrum

of  $\text{Mg}^+(\text{NH}_3)_4$  (Fig. 4a). Then we use the argon tagging method to obtain the spectrum shown in Fig. 4b. An intense band is found at  $3204\text{ cm}^{-1}$  with shoulders on both sides and weaker bands are seen at  $3270$ ,  $3318$ , and  $3366\text{ cm}^{-1}$ .

All the transitions appearing in the theoretical spectra of 4I and 4II (Figs. 4c and d) are due to the free NH stretches of the ammonia molecules directly bonded to  $\text{Mg}^+$ . In the spectrum of 4III (Fig. 4e), on the other hand, a hydrogen-bonded NH stretch is located at  $2962\text{ cm}^{-1}$  in addition to the free NH stretches in the  $3240\text{--}3410\text{ cm}^{-1}$  region. On a cursory glance at structure 4IV, the fourth ammonia molecule seems to be hydrogen-bonded to the two molecules in the first shell. As seen in Fig. 4f, however, the NH stretches involved in the hydrogen bonds ( $3202$  and  $3217\text{ cm}^{-1}$ ) show neither significant red shifts nor enhanced intensities. The intermolecular bonds between the ammonia molecules in 4IV are not so strong as anticipated from its apparent structure.

The experimental spectrum of  $\text{Mg}^+(\text{NH}_3)_4$  (Fig. 4a) displays no noticeable absorption in the region of the hydrogen-bonded NH stretch of 4III, indicating that 4III is missing under the present experimental conditions. However, it is not straightforward to discriminate among structures 4I, 4II, and 4IV, because the lowest-frequency ones of the free NH stretches of 4I and 4II (at  $3148$  and  $3179\text{ cm}^{-1}$ , respectively) are located at positions similar to the hydrogen-bonded NH stretches of 4IV. So if we suppose that the number of the solvent molecules that can be directly bonded to  $\text{Mg}^+$  is limited to three, as observed in  $\text{Mg}^+(\text{H}_2\text{O})_n$  [25] and  $\text{Mg}^+(\text{CH}_3\text{OH})_n$  [26], then 4IV is the only candidate for  $\text{Mg}^+(\text{NH}_3)_4$ . In the theoretical spectrum of 4IV, the intensity of the  $3342\text{ cm}^{-1}$  band in the higher-frequency subgroup is comparable to that of the  $3217\text{ cm}^{-1}$  band in the lower-frequency subgroup of the transitions. In contrast, the  $3204\text{ cm}^{-1}$  band in the experimental spectrum of  $\text{Mg}^+(\text{NH}_3)_4\text{-Ar}$  is much stronger than the other ones in the higher-frequency region. As far as the relative intensities of the bands are concerned, the spectrum of 4IV disagrees with the experimental observation. Therefore it is not appropriate to attribute all the features seen in Fig. 4b to 4IV alone. The outstanding intensity of the  $3204\text{ cm}^{-1}$  band is indicative of 4I and/or 4II, because the position is consistent with the  $3148$  and  $3179\text{ cm}^{-1}$  transitions of 4I and 4II, respectively.

### 3.5. $Mg^+(NH_3)_5$

The three lowest-frequency transitions in the theoretical spectrum of 5I (Fig. 5b) are anomalously strong, although they originate from the free NH stretches. In the spectra of 5II and 5III (Figs. 5c and 5d), on the other hand, the intensity of the hydrogen-bonded NH stretches located below  $3000\text{ cm}^{-1}$  is extremely weak, in contrast to 3II and 4III, where the hydrogen-bonded NH stretch is by far the most intense transition in each spectrum. Instead, the free NH stretches with the lowest-frequency are considerably strong in the spectra of 5II and 5III. Hydrogen-bonded NH stretches of 5IV at  $3178$  and  $3185\text{ cm}^{-1}$  (Fig. 5e) do not show large red shifts, as in the case of 4IV, but the intensity of the former transition is enhanced significantly. The spectra of 3+2 structures (not shown) display two intense transitions below  $3000\text{ cm}^{-1}$ , which are due to hydrogen-bonded NH stretches.

The solvation through a single hydrogen bond manifests itself as the NH stretch transition below  $3000\text{ cm}^{-1}$ , as demonstrated for 5II and 5III. The absence of palpable absorption in this region of the experimental spectrum (Fig. 5a) suggests that structures 5II and 5III are insignificant under our experimental conditions. However, we must be careful in discarding 5II, because the intensity calculated for the hydrogen-bonded NH stretch is considerably small relative to the strongest transitions around  $3132\text{ cm}^{-1}$ . Meanwhile, the theoretical spectra of both 5I and 5IV agree with the experimental spectrum, where the transitions in the  $3100\text{--}3200\text{ cm}^{-1}$  region are overwhelmingly stronger than the others. Although 5I is a 5+0 structure and 5IV is a 4+1 structure, the spectral patterns of 5I and 5IV are quite similar to each other. The similarity makes it difficult to discriminate between the two structures through the IR spectroscopy.

The most important conclusion to be drawn from these results is that at least four ammonia molecules can be directly bonded to  $Mg^+$ , in striking contrast to the  $Mg^+(H_2O)_n$  system where the first solvent shell is filled with three water molecules.

### 3.6. Solvation structures

Bohme et al. [12] carried out multi-CID experiments using a selected ion flow tube (SIFT) apparatus operated at room temperature. They interpreted the inflection observed in the CID profile of  $\text{Mg}^+(\text{NH}_3)_3$  in terms of the presence of two isomers. They argued that the sterically less hindered 2+1 structure was dominant over the 3+0 structure.

Fuke et al. [18] examined the photodissociation spectra of  $\text{Mg}^+(\text{NH}_3)_n$  ( $n = 1-4$ ) in the 9000–41000  $\text{cm}^{-1}$  region to explore the stepwise change in the electronic structure of the  $\text{Mg}^+$  chromophore. The spectra exhibit increasing red shifts with cluster size from  $n = 1$  to 3. The  $n = 4$  spectrum displays broad bands around 10000 and 14000  $\text{cm}^{-1}$  with a tail extending to 32500  $\text{cm}^{-1}$ . Both bands are further red-shifted from the  $n = 3$  band, suggesting that the fourth molecule still perturbs the electronic structure of  $\text{Mg}^+$ . With assistance from theoretical calculations, Fuke et al. assigned the 10000 and 14000  $\text{cm}^{-1}$  bands to the transitions of the 4+0 structures (4I and 4II, respectively). Meanwhile, the 20000–25000  $\text{cm}^{-1}$  region of the tail, where the  $n = 3$  spectrum shows a strong absorption, was attributed to the 3+1 structures (4III and 4IV). Farrar et al. [9] extended the measurement of the spectra up to  $n = 7$ . They supported the previous interpretation that the 4+0 structures dominantly contribute to the  $n = 4$  spectrum, but made no reference to the 3+1 structures. The spectra of  $n = 5-7$  strongly resemble that inferred for the lowest-energy feature of  $n = 4$ ; the sharply rising edge near 9000  $\text{cm}^{-1}$  in the  $n = 4$  spectrum also appears in the spectra of the next three clusters. Farrar et al. suggested that the first solvation shell is filled with four ammonia molecules and that 4I forms the most stable core on which to build the second solvation shell.

The present study demonstrates that IR spectroscopy enables us to investigate the solvation structures by probing hydrogen-bonding interactions among the solvent molecules through the NH stretches of ammonia. The  $n = 3$  spectrum proves that the  $\text{Mg}^+(\text{NH}_3)_3$  ions produced in our cluster source have exclusively the 3+0 structure, as opposed to the argument made by Bohme and co-workers. The discrepancy is attributable to the large difference in the experimental conditions between the two studies. The  $n = 4$  spectrum indicates that the coexistence of 4III is unlikely, although Fuke et al. suggested that all of 4I–4IV contribute to the electronic spectrum of  $n = 4$ . The present IR spectra as well as the previous electronic

spectra [9,18] indicate that the 4+0 structures are the dominant forms of  $\text{Mg}^+(\text{NH}_3)_4$ , in striking contrast to the 3+1 structures of  $\text{Mg}^+(\text{H}_2\text{O})_n$  [25] and  $\text{Mg}^+(\text{CH}_3\text{OH})_n$  [26].

Farrar et al. suggested the core of 4I form in the  $n \geq 5$  clusters on the basis of the electronic spectra. If this suggestion holds true, the most probable form of  $n = 5$  would be 5II, since the 4I core is retained only in 5II from our DFT calculations. However, the spectral feature characteristic of 5II is not clearly observed in the experimental spectrum. Instead, the spectra of both 5I and 5IV are consistent with the experimental results. It is necessary, therefore, to ascertain whether these structures are consistent with the electronic spectrum reported by Farrar et al. Theoretical calculations of the electronic transition energies for the  $n = 5$  clusters will be helpful in resolving the issues of the solvation structures comprehensively. In any case, the IR spectrum of  $n = 5$  reveals that even the fifth ammonia molecule may possibly be bonded to  $\text{Mg}^+$  directly, to say nothing of the fourth one.

Finally, let us compare the solvation structures of  $\text{Mg}^+(\text{NH}_3)_n$  and  $\text{Mg}^+(\text{H}_2\text{O})_n$ . Stace et al. [27] found that the fifth water molecule in  $\text{Cu}^{2+}(\text{H}_2\text{O})_5$  prefers a hydrogen bonded site in the second shell rather than direct attachment to the metal ion. They attributed this preference to the following two factors. Firstly, the high charge density on the  $\text{Cu}^{2+}$  ion will polarize water molecules in the first shell. As a result, ‘charge-enhanced’ hydrogen bonds will be formed, which are stronger than those associated with neutral systems. Secondly, the lone-pair electrons on the fifth molecule in the second shell form double-acceptor hydrogen bonds, which bridge two water molecules in the first shell. Similarly, the fourth water molecule in  $\text{Mg}^+(\text{H}_2\text{O})_4$  prefers the solvation through double-acceptor hydrogen bonds rather than the direct coordination with the  $\text{Mg}^+$  ion, but that is not the case for  $\text{Mg}^+(\text{NH}_3)_4$ . This means that the size of the first shell is not inherent in the  $\text{Mg}^+$  ion, but is variable depending on the solvent molecules. As there are two lone pairs on the oxygen atom in contrast to the single lone pair on the nitrogen atom, the double-acceptor hydrogen bonds in  $\text{Mg}^+(\text{H}_2\text{O})_4$  are expected to be stronger than those in 4IV of  $\text{Mg}^+(\text{NH}_3)_4$ . Because of the charge enhancement, the hydrogen-bonding interaction in  $\text{Mg}^+(\text{H}_2\text{O})_4$  is relatively strong compared to the direct interaction between the fourth water molecule and the  $\text{Mg}^+$  ion, having a

preference for the 3+1 structure. On the other hand, the dissociation energy of  $\text{Mg}^+-\text{NH}_3$  ( $1.60\pm 0.12$  eV) is measured to be larger than that of  $\text{Mg}^+-\text{H}_2\text{O}$  ( $1.23\pm 0.13$  eV) [15], indicating the stronger ion–solvent interaction in the former system. Thus the difference in the solvation structures between  $\text{Mg}^+(\text{NH}_3)_n$  and  $\text{Mg}^+(\text{H}_2\text{O})_n$  probably originates in the relative magnitude of the ion–solvent and solvent–solvent interactions. It is concluded that the size of the first solvent shell is smaller for those molecules which have a propensity to form stronger hydrogen bonds.

### Acknowledgement

We thank Dr. K. Ohshimo for his help in equipping our photodissociation spectrometer with the laser vaporization source. This work was supported in part by the Joint Studies Program (2003) of the Institute for Molecular Science and the Grant-in-Aid for Scientific Research (No. 15250015) from the Ministry of Education, Culture, Sports, Science, and Technology of Japan.

### References

- [1] A. W. Castleman, Jr., K. H. Bowen, *J. Phys. Chem.* 100 (1996) 12911.
- [2] P. Kebarle, *Ann. Rev. Phys. Chem.* 28 (1977) 445.
- [3] A. W. Castleman, Jr., R. G. Keesee, *Chem. Rev.* 86 (1986) 589.
- [4] T. D. Märk, *Int. J. Mass Spectrom. Ion Processes* 79 (1987) 1.
- [5] J. M. Lisy, *Int. Rev. Phys. Chem.* 16 (1997) 267.
- [6] G. Gregoire, M. A. Duncan, *J. Chem. Phys.* 117 (2002) 2120.
- [7] R. S. Walters, T. D. Jaeger, M. A. Duncan, *J. Phys. Chem. A* 106 (2002) 10482.
- [8] K. Fuke, K. Hashimoto, S. Iwata, *Adv. Chem. Phys.* 110 (1999) 431.
- [9] J. M. Farrar, *Int. Rev. Phys. Chem.* 22 (2003) 593.
- [10] C. W. Bauschlicher, Jr., H. Partridge, *Chem. Phys. Lett.* 181 (1991) 129.
- [11] C. W. Bauschlicher, Jr., M. Sodupe, H. Partridge, *J. Chem. Phys.* 96 (1992) 4453.
- [12] R. K. Milburn, V. I. Baranov, A. C. Hopkinson, D. K. Bohme, *J. Phys. Chem. A* 102

(1998) 9803.

[13] T. Shoeib, R. K. Milburn, G. K. Koyanagi, V. V. Lavrov, D. K. Bohme, K. W. M. Siu, A. C. Hopkinson, *Int. J. Mass Spectrom.* 201 (2000) 87.

[14] R. K. Milburn, D. K. Bohme, A. C. Hopkinson, *J. Mol. Struct. (Theochem)* 540 (2001) 5.

[15] A. Andersen, F. Muntean, D. Walter, C. Rue, P. B. Armentrout, *J. Phys. Chem. A* 104 (2000) 692.

[16] M. Elhanine, L. Dukan, P. Maître, W. H. Breckenridge, S. Massick, B. Soep, *J. Chem. Phys.* 112 (2000) 10912.

[17] S. Yoshida, N. Okai, K. Fuke, *Chem. Phys. Lett.* 347 (2001) 93.

[18] S. Yoshida, K. Daigoku, N. Okai, A. Takahata, A. Sabu, K. Hashimoto, K. Fuke, *J. Chem. Phys.* 117 (2002) 8657.

[19] Y. Inokuchi, N. Nishi, *J. Chem. Phys.* 114 (2001) 7059.

[20] M. B. Knickelbein, W. J. C. Menezes, *Phys. Rev. Lett.* 69 (1992) 1046.

[21] P. Ayotte, G. H. Weddle, J. Kim, M. A. Johnson, *Chem. Phys.* 239 (1998) 485.

[22] N. L. Pivonca, C. Kaposta, M. Brümmer, G. von Helden, G. Meijer, L. Wöste, D. M. Neumark, K. R. Asmis, *J. Chem. Phys.* 118 (2003) 5275.

[23] G. Gregoire, N. R. Brinkmann, D. van Heijnsbergen, H. F. Schaefer, M. A. Duncan, *J. Phys. Chem. A* 101 (1997) 2279.

[24] M. J. Frisch et al., Gaussian, Inc., Pittsburgh PA, 1998.

[25] Y. Inokuchi, K. Ohshimo, F. Misaizu, N. Nishi, *J. Phys. Chem. A* (in press).

[26] H. Machinaga, K. Ohashi, Y. Inokuchi, N. Nishi, H. Sekiya, *Chem. Phys. Lett.* 391 (2004) 85.

[27] A. J. Stace, *Phys. Chem. Chem. Phys.* 3 (2001) 1935.

## Figure Captions

Fig. 1. Stable structures of  $\text{Mg}^+(\text{NH}_3)_n$  with (a)  $n = 3$ , (b)  $n = 4$ , and (c)  $n = 5$  obtained from DFT calculations at the B3LYP/6-31+G\* level. Magnesium and nitrogen atoms are denoted by solid and shaded circles, respectively.

Fig. 2. IR photodissociation spectra of  $\text{Mg}^+(\text{NH}_3)_n$  ( $n = 3-6$ ) in the  $2600-3600 \text{ cm}^{-1}$  region. Amplitude of four spectra is normalized independently at each maximum.

Fig. 3. Experimental IR spectra of (a)  $\text{Mg}^+(\text{NH}_3)_3$  reproduced from Fig. 2a and (d)  $\text{Mg}^+(\text{NH}_3)_3\text{-Ar}$ . Theoretical IR spectra obtained from DFT calculations for (b) 3I and (c) 3II. Intensity of the spectrum of 3I is magnified by a factor of 10.

Fig. 4. Experimental IR spectra of (a)  $\text{Mg}^+(\text{NH}_3)_4$  reproduced from Fig. 2b and (b)  $\text{Mg}^+(\text{NH}_3)_4\text{-Ar}$ . Theoretical IR spectra obtained from DFT calculations for (c) 4I, (d) 4II, (e) 4III, and (f) 4IV. Intensity of the spectrum of 4IV is magnified by a factor of 5.

Fig. 5. (a) Experimental IR spectrum of  $\text{Mg}^+(\text{NH}_3)_5$  reproduced from Fig. 2c. Theoretical IR spectra obtained from DFT calculations for (b) 5I, (c) 5II, (d) 5III, and (e) 5IV.

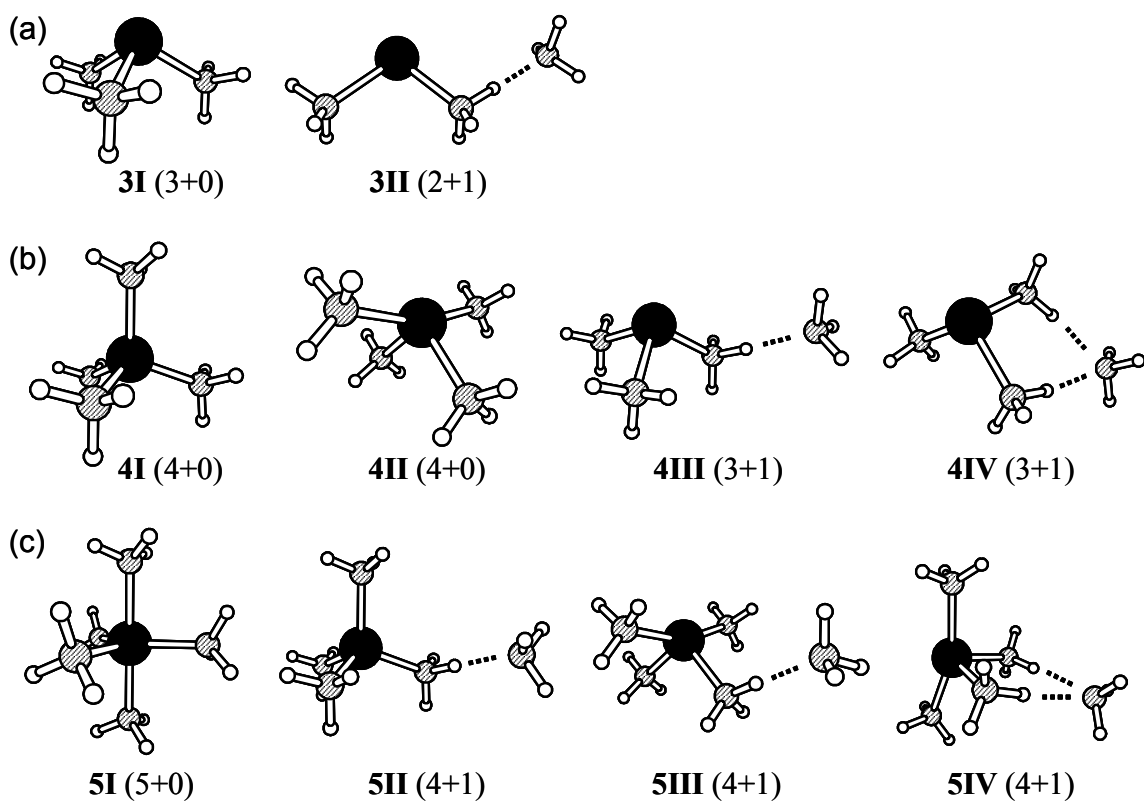


Fig. 1 Ohashi et al.

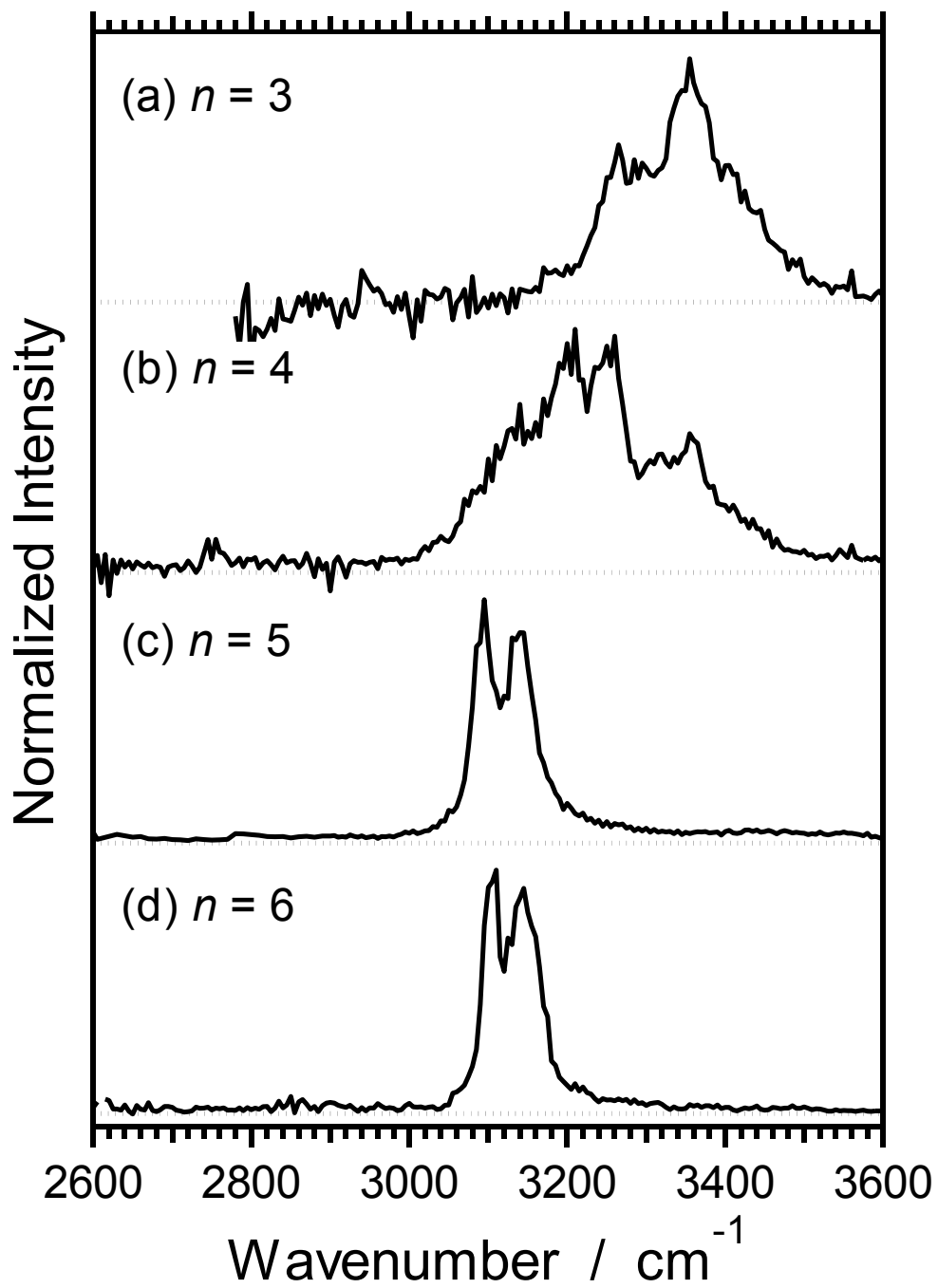


Fig. 2 Ohashi et al.

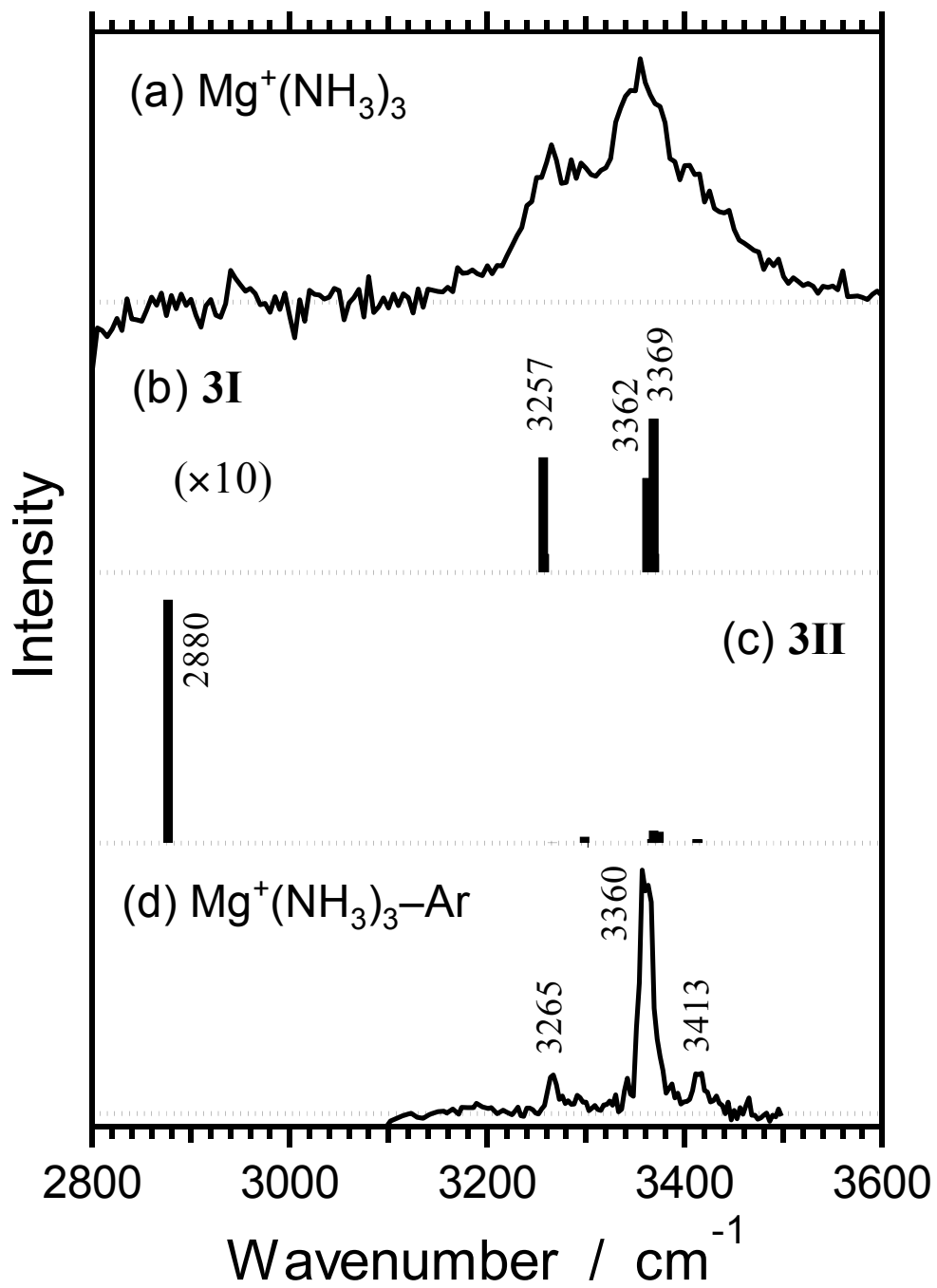


Fig. 3 Ohashi et al.

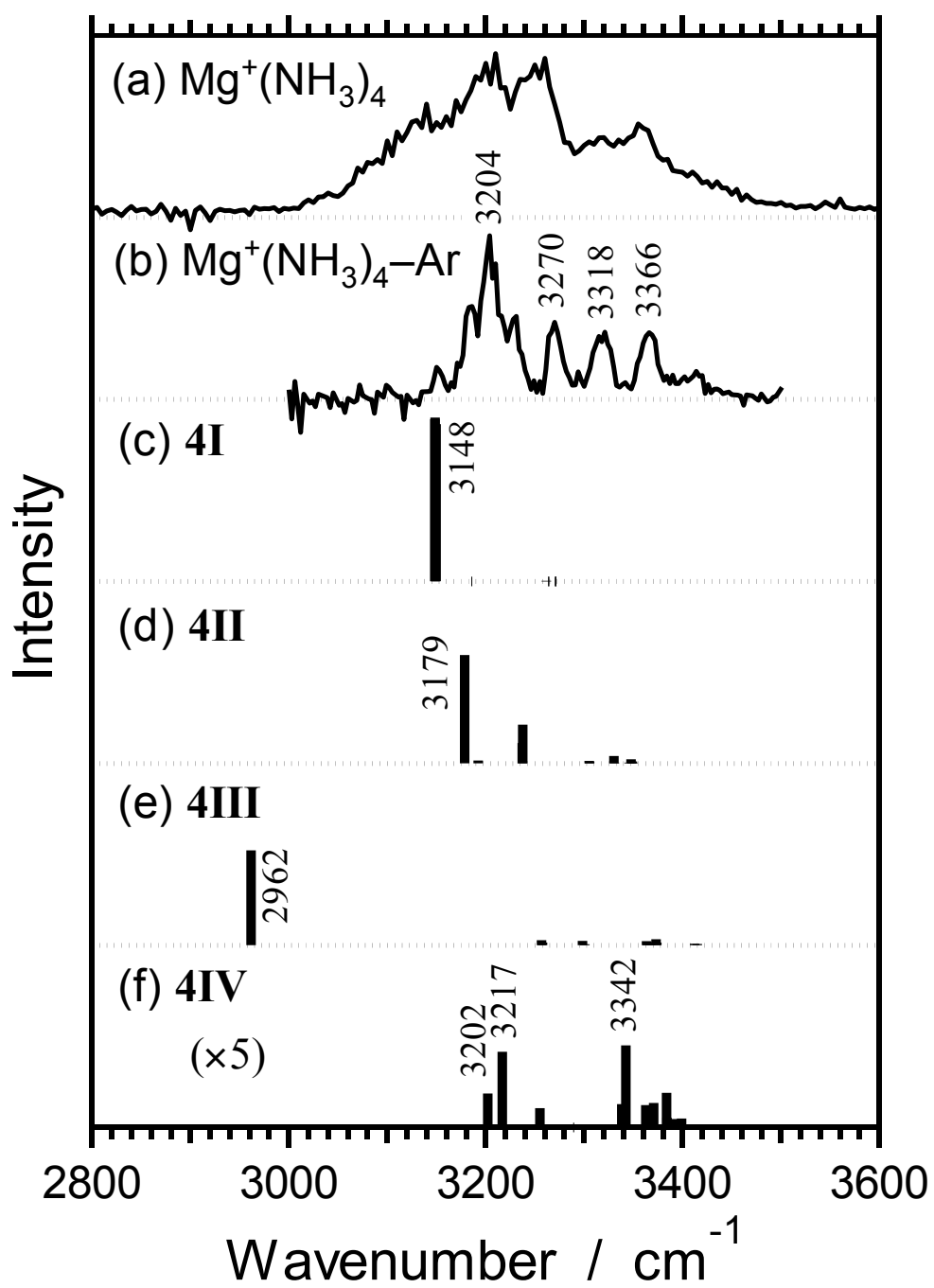


Fig. 4 Ohashi et al.

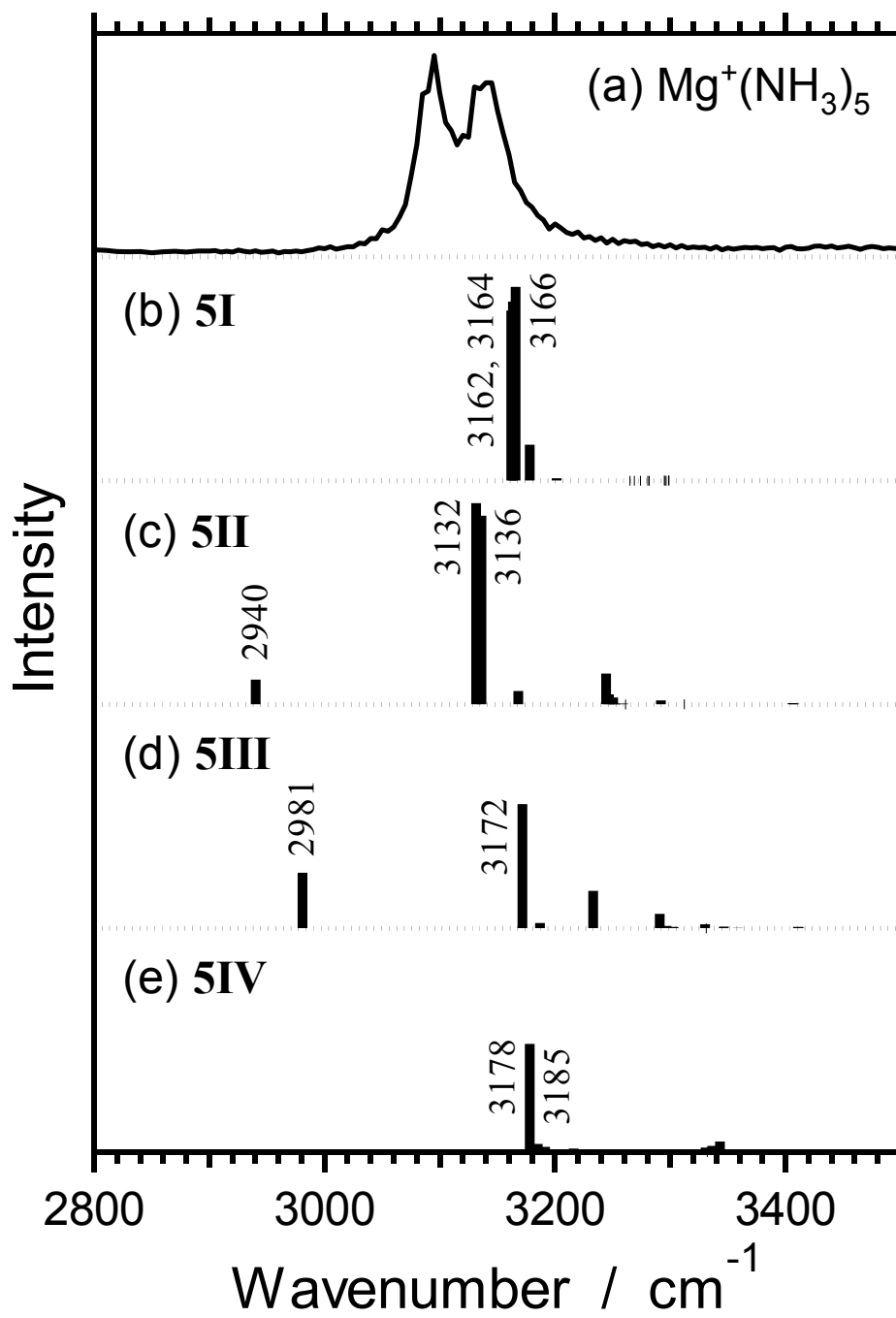


Fig. 5 Ohashi et al.

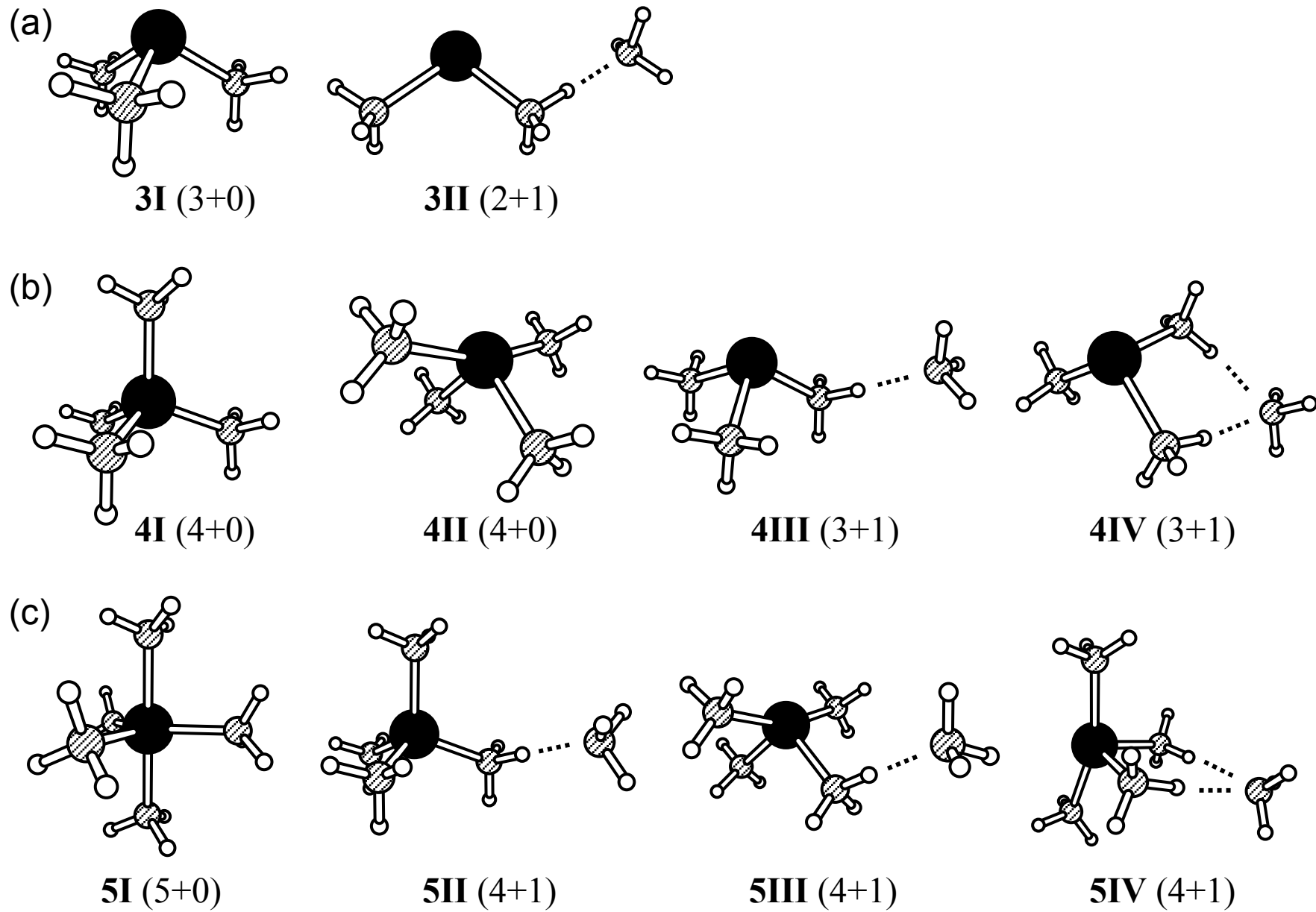


Fig. 1 Ohashi et al.

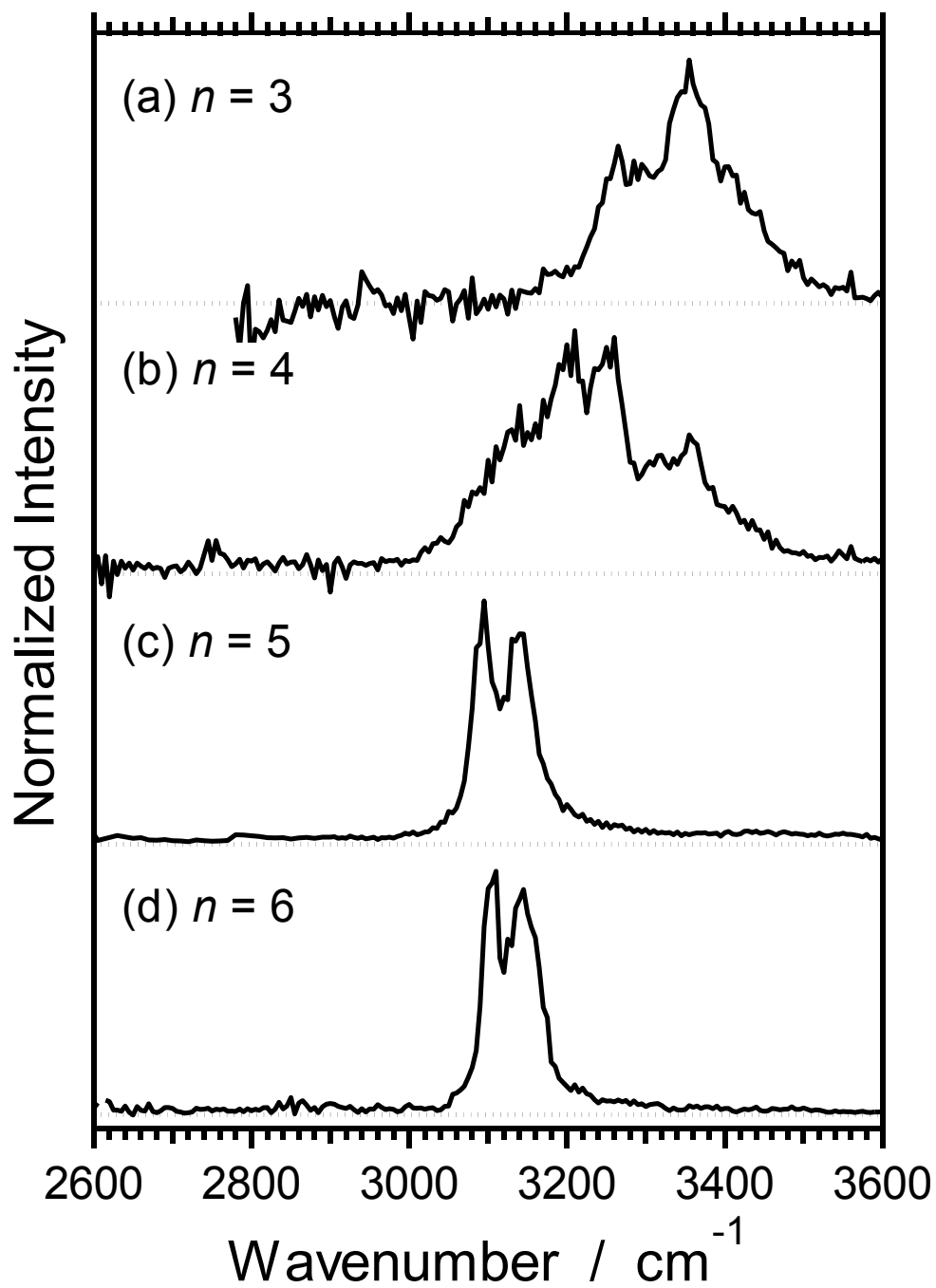


Fig. 2 Ohashi et al.

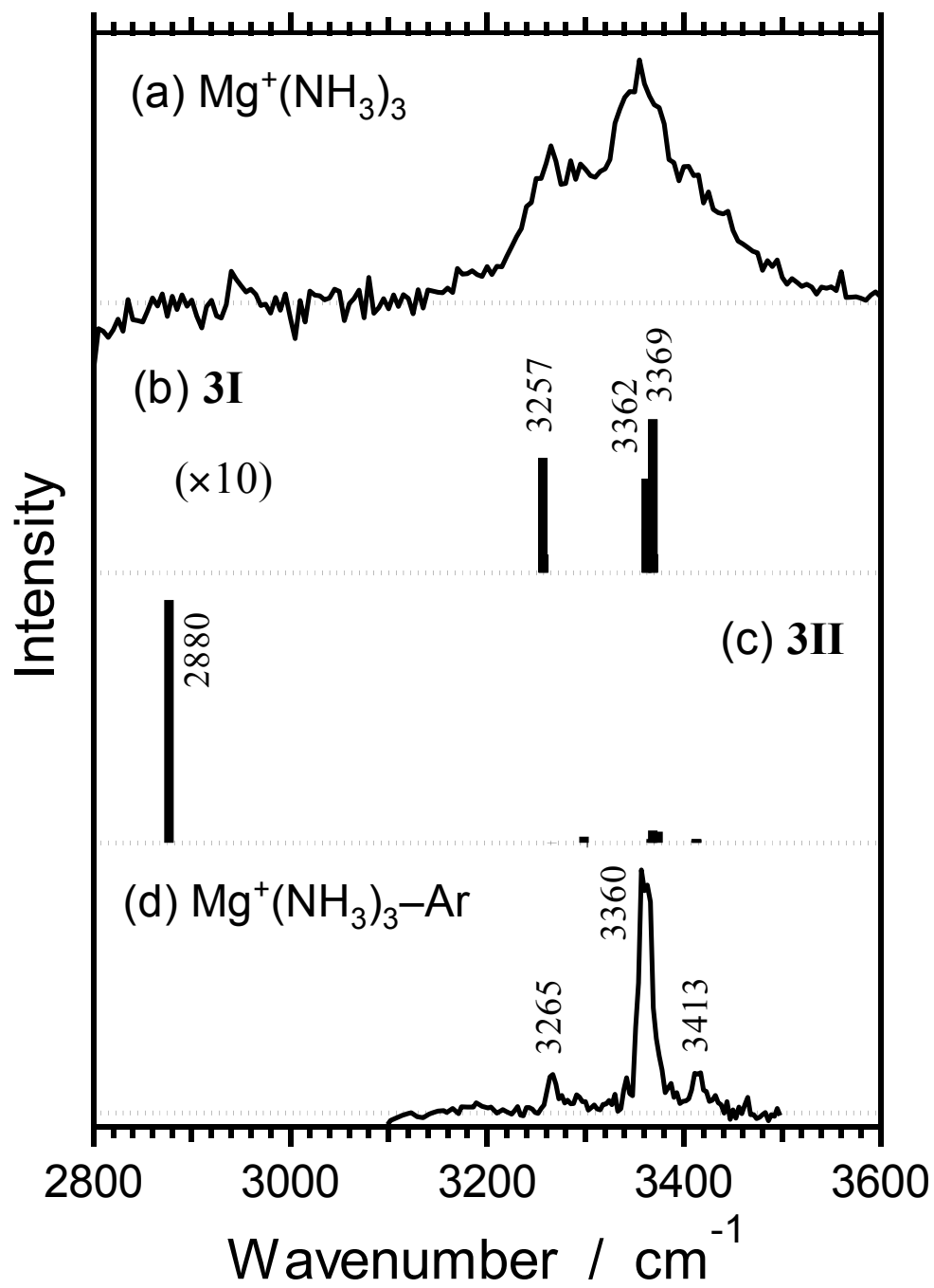


Fig. 3 Ohashi et al.

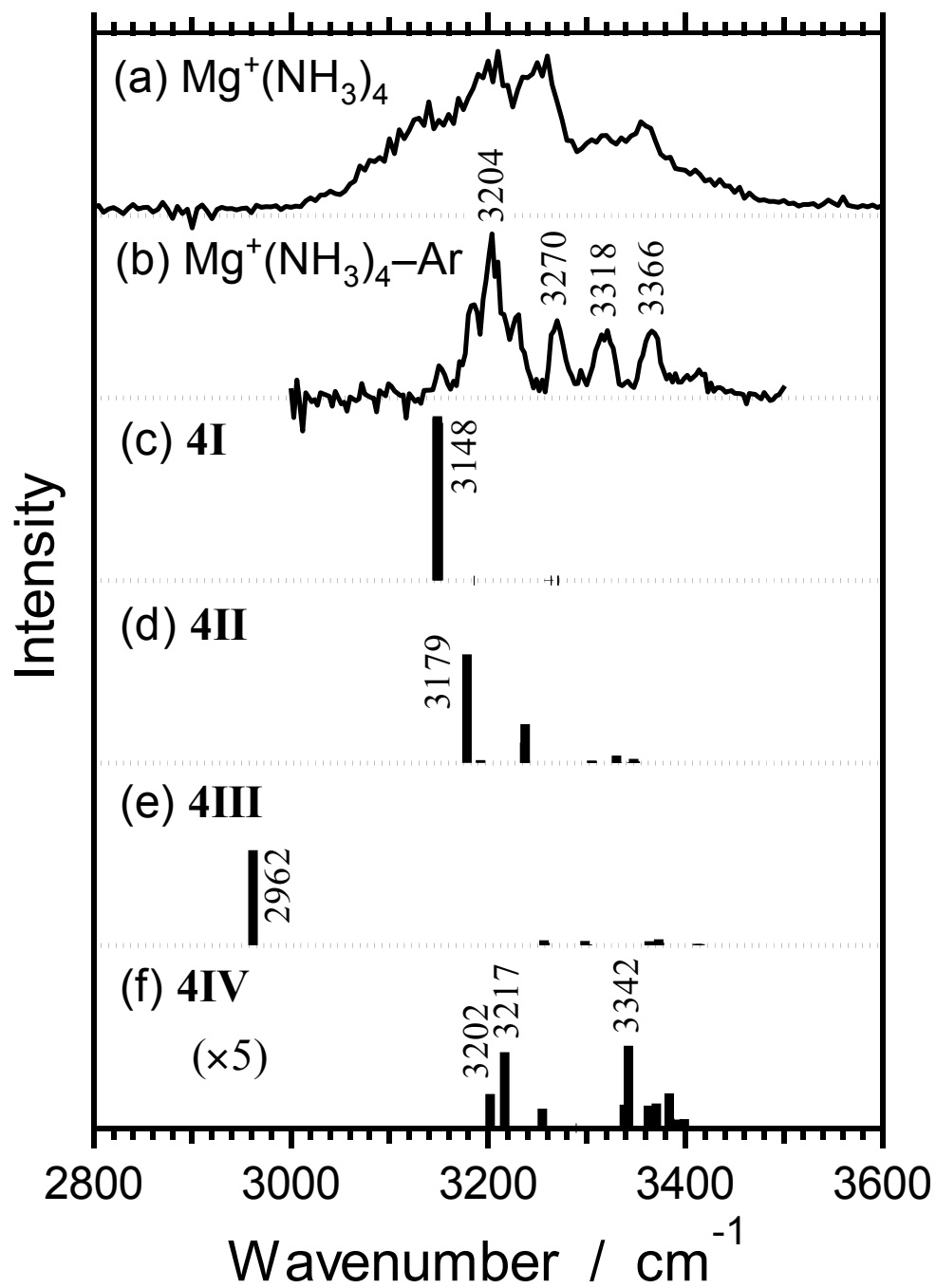


Fig. 4 Ohashi et al.

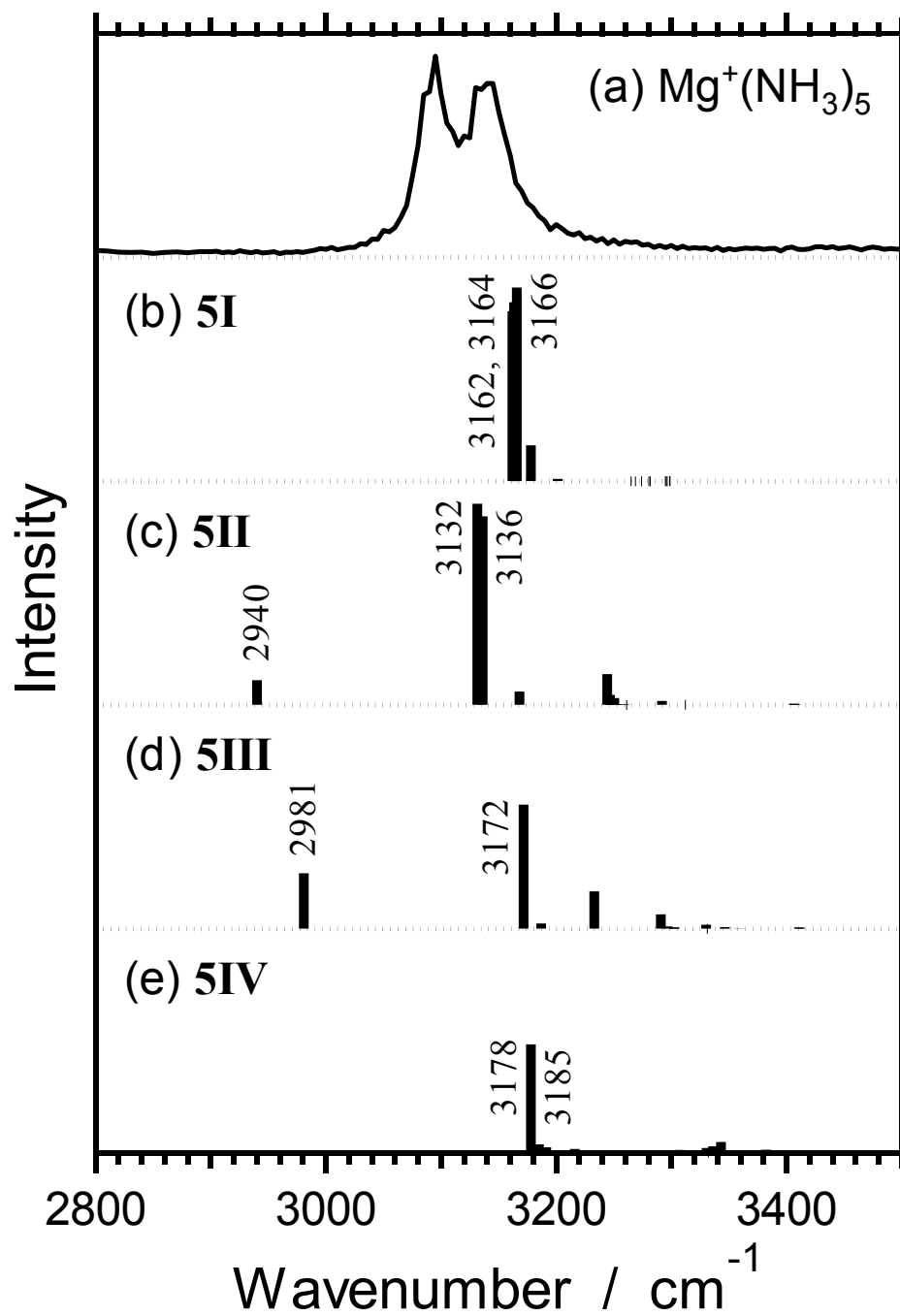


Fig. 5 Ohashi et al.